Mathematical Biosciences 283 (2017) 48–59

Contents lists available at ScienceDirect

Mathematical Biosciences

journal homepage: www.elsevier.com/locate/mbs

Mathematical model of Ebola transmission dynamics with relapse and reinfection

F.B. Agusto

Department of Ecology and Evolutionary Biology, University of Kansas, Lawrence, KS, United States

ARTICLE INFO

Article history:
Received 5 April 2016
Revised 27 August 2016
Accepted 1 November 2016
Available online 8 November 2016

MSC:
92B05
93A30
93C15

Keywords:
Ebola
Relapse
Reinfection
Backward bifurcation
Sensitivity analysis
Control intervention

ABSTRACT

The Ebola virus disease is caused by the Ebola virus which belongs to the *filoviridae* virus family. The 2014 outbreaks were estimated to have caused over 11,000 fatalities. In this paper, we formulate and analyze a system of ordinary differential equations which incorporates disease relapse and reinfection. The Ebola model with disease relapse and reinfection is locally-asymptotically stable when the *basic reproduction number* is less than unity. The model exhibits in the presence of disease reinfection, the phenomenon of backward bifurcation, where the stable disease-free equilibrium co-exists with a stable endemic equilibrium when the associated reproduction number is less than unity. The feasibility of backward bifurcation occurring increases with increasing values of both relapse and reinfection. The total number of new cases of Ebola-infected individuals increases with increasing values of the relapse and reinfection parameters. Further simulations show that Ebola transmission models that do not incorporate relapse and reinfection may under-estimate disease burden in the community. Similar under-estimation is observed in models that include only one infected and recovered classes. Using results obtained from sensitivity analysis indicates that Ebola (given disease relapse and reinfection) can be effectively curtailed in the community by using control measures with a high-effectiveness level. This strategy is more effective than either the moderate- or low-effectiveness levels.

1. Introduction

The Ebola virus is caused by the Ebola Virus Disease (EVD); it belongs to the *filoviridae* virus family. It is transmitted person-to-person *via* direct contact with infected bodily fluids, secretions, organs, blood, and contaminated surfaces and materials [44]. The EVD case fatality varied from 25% to 90%, however, the case fatality rate on average is around 50% [44]. The 2014 West Africa EVD outbreak had case fatality rate of about 50% and it was the largest and most devastating Ebola outbreak since the first known outbreaks in 1976 [44], which occurred in Sudan and in the Democratic Republic of Congo (the later outbreak was identified near the Ebola River, where the disease got its name [11,42]). The 2014 EVD outbreak (believed to have started in Guinea in March 2014 [42] is the first to have occurred in West Africa [12]). It ravaged three countries (Guinea, Liberia, and Sierra Leone) and further spread by air and land travels to Nigeria, USA , Senegal and Mali [44].

The incubation period of EBOV is between 2 and 21 days [14,16,42] (some studies have estimated the most common incubation period to be 8–10 days [13]). Ebola-infected humans typically exhibit flu-like symptoms during the first 1–3 days of the infection [14], and can thereafter have, or progress to, other symptoms such as fever, severe headache, muscle aches, weakness, vomiting, diarrhea, stomach pains, loss of appetite and at times bleeding (which may be visible or internal) [13,14,43]. The infected human is capable of transmitting the disease to susceptible individuals at the onset of symptoms [14,42].

Following the 2014 outbreak, Liberia was first declared Ebola free in May 2015. The virus was, however, re-introduced twice, with the latest flare-up in November 2015 [46]. To date, 10 such flare-ups which were not part of the original 2014 outbreak were identified, and these are likely the result of the virus persisting in survivors even after recovery [46]. Evidence shows that the virus disappears relatively quickly from survivors, but can remain in the semen of a small number of male survivors for as long as 1 year, and in rare instances, be transmitted to intimate partners [46]. A number of studies [6,17,25,34,35,41,45] show that Ebola virus can persist in testes, spinal cord and eye chamber, sweat, breast milk, aqueous humor, semen, vaginal fluids, urine, amniotic fluid, the placenta and the central nervous system of survivors. During the 1995 Kikwit outbreak [34], a patient had live virus isolated from the seminal fluid 82 days after disease onset. In another study [17], Ebola virus RNA was shown to be present in the semen of survivors for 2 to 9 months post-onset of EVD, [45]. EVD was also

E-mail address: fbagusto@gmail.com

http://dx.doi.org/10.1016/j.mbs.2016.11.002
0025-5564/

shown to be present in sweat and urine for up to 40 days and in urine culture for 26 days after disease symptoms onset [25]. The persistence of EVD virus poses major risks to the survivors and the community [[29]]. It may lead to reactivation (i.e. relapse) of the illness in affected individuals and onward transmission to others either asymptomatically or symptomatically [[29]]. Animal studies support persistence of Ebola virus and subsequent re-emergence of symptoms [22,37].

Recovery from EVD requires both humoral and cell-mediated immunity [[29]], and there is variability in individuals immune response and between EVD outbreaks [36]. Furthermore, variability in host immunity can determine the susceptibility of the host to reinfection [22]. Recovered mice, who were reinfected with the virus developed lethal infection due to the development of partial immunity [22]. In the trial of ZMab in macaques, 2 of 12 monkeys who had lower immunity succumbed to a reinfection [39]. However, individuals with a more robust immune system, develop subclinical or asymptomatic infection [23,28]. For instance, the virus was detected through PCR in two children in Monrovia, who had recovered clinically and had a negative PCR result at the time of discharge [[29]]. Also, a group of women in Guinea despite repeated exposure to the virus were not infected, with just one of them having the Ebola virus antibodies in her blood [21]. Thus, these points to variability in individual host susceptibility to infection and reinfection, based on the host innate immunity as well as the viral load they are exposed to during an infection or reinfection [[29]].

The Ebola epidemic claimed the lives of more than 11,300 people and infected over 28,500. The disease wrought devastation on families, communities and the health and economic systems of the 3 most affected countries (Guinea, Liberia and Sierra Leone) [46]. According to the World Health Organization, the risk of re-introduction of infection is diminishing as the virus gradually clears from the survivor population, but more flare-ups are still anticipated [46] and that strong surveillance and response systems will be critical in the months to come. Thus, the purpose of the current study is to assess the impact of relapse and reinfection of Ebola on the transmission dynamics of EVD in a population. To achieve this objective, a new deterministic compartmental model, which incorporates the above features and other pertinent epidemiological, demographic and biological aspects of EVD, will be designed and the theoretical properties will be investigated.

A number of mathematical models and statistical methods have been used in an attempt to understand the transmission dynamics of EVD (see, for instance, [3,4,16,20,26,32,38], and some of the references therein). In [16], a compartmental mathematical model was used to estimate the number of secondary cases generated by an index case, in the absence or presence of control measures, for the 1995 Congo and 2000 Uganda Ebola outbreaks. The study further highlighted the importance of basic public health control measures, such as public health education, contact tracing and quarantine of suspected cases, and the role such measures can play in reducing the final size of the epidemics. Most recently, the basic reproduction number for the 2014 Ebola outbreak was estimated in [3,4,20,30,32,38]. Agusto et al. [3], using incidence data from Guinea estimated $\mathcal{R}_0$ for EBOV and investigated the impact of non-pharmaceutical control measures. Their study shows that the disease incidence can be reduced by simple use of non-pharmaceutical measures sure as increasing the duration of healthcare workers' daily work shifts; limiting the length of hospital visitation of members of the public and effectively educating the populace to desist from practicing traditional/cultural beliefs system and customs that aid the spread of Ebola in the affected regions. Althaus [4] estimated $\mathcal{R}_0$ for EBOV using incidence data and a SEIR model. The study emphasizes the heightening of control measures in the three countries (especially in Liberia). Legrand et al. [26], developed a compartmental model, using data from 1995 Democratic Republic of Congo (DRC) and 2000 Uganda epidemic, which allow for EBOV transmission by infected people in the community and in the hospital.

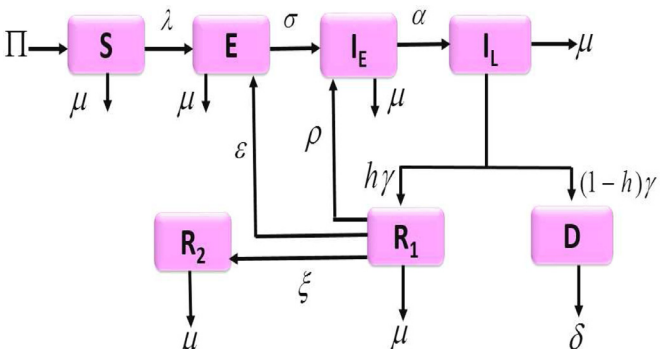

Fig. 1. Flow diagram of the Ebola transmission model.

The paper is organized as follows. The model is formulated in Section 2. In Section 3, we investigate the theoretical properties of the Ebola model with relapse and reinfection and carry out numerical exploration of the model in Section 4. Discussion and conclusions of this study are stated in Section 6.

2. Model formulation

We model the transmission dynamics of the Ebola virus disease (EVD) extending the compartmental framework of the pre-intervention model presented in [3]. The total population, $N_H(t)$, at time t is split into mutually-exclusive sub-populations of individuals who are susceptible ($S(t)$), exposed ($E(t)$), symptomatic individuals in the early-stage of EVD infection ($I_E(t)$), symptomatic individuals in the late-stage of EVD infection ($I_L(t)$), recovered and immune individuals ($R_1(t), R_2(t)$) and Ebola-infected deceased individuals ($D(t)$). So that

$$N(t) = S(t) + E(t) + I_E(t) + I_L(t) + R_1(t) + R_2(t) + D(t)$$

The equations of the mathematical model are given below. The flow diagram of the model is depicted in Fig. 1, and the associated state variables and parameters are described in Table 1.

$$\begin{aligned}
\dot{S}(t) &= \Pi - \lambda(I_E, I_L, R_1, D)S(t) - \mu S(t),\\
\dot{E}(t) &= \lambda(I_E, I_L, D)S(t) + \varepsilon\lambda(I_E, I_L, R_1, D)R_1(t) - (\sigma + \mu)E(t),\\
\dot{I}_E(t) &= \sigma E(t) - (\alpha + \mu)I_E(t) + \rho R(t),\\
\dot{I}_L(t) &= \alpha I_E(t) - (\gamma + \mu)I_L(t),\\
\dot{R}_1(t) &= h\gamma I_L(t) - (\rho + \xi + \mu)R_1(t) - \varepsilon\lambda(I_E, I_L, R_1, D)R_1(t),\\
\dot{R}_2(t) &= \xi R_1(t) - \mu R_2(t),\\
\dot{D}(t) &= (1-h)\gamma I_L(t) - \delta D(t),
\end{aligned} \tag{2.1}$$

where,

$$\lambda(I_E, I_L, R_1, D) = \frac{\beta(I_E + I_L + \tau_1 R_1 + \tau_2 D)}{S + E + I_E + I_L + R_1 + R_2 + D}$$

is the infection rate of the disease, and all other parameters are as defined on Table 1. In particular, β is the effective contact (transmission) rate, τ_1 and τ_2 are modification parameters that account

Table 1
Description of the state variables and parameters of the Ebola model (2.1).

Variable	Description
$S(t)$	Population of susceptible individuals
$E(t)$	Population of exposed individuals
$I_E(t)$	Population of symptomatic individuals in the early-stage of EBOV infection
$I_L(t)$	Population of symptomatic individuals in the late-stage of EBOV infection
$R_1(t), R_2(t)$	Population of recovered and immune individuals
$D(t)$	Population of Ebola-deceased individuals
Parameter	Description
β	Effective contact (transmission) rate
Π	Recruitment rate
μ	Natural death rate
τ	Modification parameters for infectiousness
ρ	Infection reactivation rate
σ	Progression rate of symptomatic individuals
α	Progression rate of early-symptomatic individuals
ξ	Progression rate of recovered individuals to immune class
h	Fraction of symptomatic individuals who recovered
ε	Reinfection modification parameters
γ	Recovery rate of symptomatic individuals
δ	Cremation/burial rate of Ebola-deceased individuals

for the assumed reduced infectiousness of the recovered individuals in the R_1 class and the Ebola-infected deceased individuals (in comparison to the living individuals with Ebola symptoms).

We have included two recovered classes $R_1(t)$ and $R_2(t)$ and assume individuals in $R_1(t)$ class can experience reinfection since the possibility of reinfection is a function of host immunity and the viral load to which an individual is exposed to or re-challenged with [[29]]. Furthermore, we assume these individuals are capable of transmitting the virus since the viruses can persist after recovery in parts of the body and could be spread through sex or other contacts with semen [10]. We also assume recovered individuals in the $R_2(t)$ class experience lifelong immunity. Studies from previous Ebola outbreaks shows antibodies to the virus could still be detected 10 years after recovery in the disease survivors [10].

The Ebola model (2.1), extends the Ebola transmission models in [4,16] and the pre-intervention model in [3] by (*inter alia*):

(i) including relapse of recovered individuals; and
(ii) including reinfection of recovered individuals; and
(iii) including two infected and recovered classes.

2.1. Basic properties

We shall now explore the basic dynamical features of model (2.1). Since the Ebola model (2.1) governs human population in the course of the Ebola epidemics, it will be epidemiologically meaningful if all its state variables are non-negative for $t \geq 0$. That is, its solution with positive initial data will remain positive for all time ($t > 0$).

Lemma 1. *Let the initial data $F(\mathbf{0}) \geq 0$, where $F(t) = (S, E, I_E, I_L, R_1, R_2, D)$. Then the solutions $F(t)$ of the Ebola model (2.1) are non-negative for all time $t > 0$. Furthermore*

$$\limsup_{t\to\infty} N(t) \leq \frac{\Pi}{\mu}$$

with,

$$N(t) = S(t) + E(t) + I_E(t) + I_L(t) + R_1(t) + R_2(t) + D(t).$$

Proof. Let $t_1 = sup\{t > 0 : F(t) > 0\}$. Thus, $t_1 > 0$. Then it follows from the first equation of the Ebola model (2.1) that

$$\frac{dS}{dt} = \Pi - \lambda(I_E, I_L, R_1, D)S - \mu S.$$

which can be re-written as

$$\frac{d}{dt}\left\{S(t)exp\left[\int_0^{t_1} \lambda(I_E(u), I_L(u), R_1(u), D(u))du + \mu t\right]\right\}$$
$$= \Pi \exp\left[\int_0^{t_1} \lambda(I_E(u), I_L(u), R_1(u), D(u))du + \mu t\right].$$

So that,

$$S(t_1)exp\left[\int_0^{t_1} \lambda(I_E(u), I_L(u), R_1(u), D(u))du + \mu t\right] - S(0)$$
$$= \Pi \exp\left[\int_0^{t_1} \lambda(I_E(u), I_L(u), R_1(u), D(u))du + \mu_H t\right].$$

Hence,

$$\begin{aligned} S(t_1) = {} & S(0)exp\left[-\int_0^{t_1} \lambda(I_E(u), I_L(u), R_1(u), D(u))du - \mu t_1\right] \\ & + \Pi \exp\left[\int_0^{t_1} \lambda(I_E(u), I_L(u), R_1(u), D(u))du + \mu t_1\right]. \\ & \times exp\left[-\int_0^{t_1} \lambda(I_E(u), I_L(u), R_1(u), D(u))du - \mu t_1\right] \\ & > 0. \end{aligned}$$

It can similarly be shown that $F > 0$ for all $t > 0$. For the second part of the proof, it should be noted that $0 < S(t) \leq N(t), 0 < E(t) \leq N(t), 0 < I_E(t) \leq N(t), 0 < I_L(t) \leq N(t), 0 < R_1(t) \leq N(t), 0 < R_2(t) \leq N(t), 0 < D(t) \leq N(t)$.

Adding the components of the model (2.1) gives

$$\frac{dN(t)}{dt} = \Pi - \mu(S + E + I_E + I_L + R_1(t) + R_2(t)) - \delta D(t). \quad (2.2)$$

For mathematical convenience, we subtract and add $\mu D(t)$ to the expression in (2.2), thus

$$\begin{aligned} \frac{dN(t)}{dt} &= \Pi - \mu[S(t) + D(t) + I_E(t) + I_L(t) + R_1(t) + R_2(t)] \\ &\quad -\mu D(t) + \mu D(t) - \delta D(t) \\ \frac{dN(t)}{dt} &= \Pi - \mu[S(t) + D(t) + I_E(t) + I_L(t) + R_1(t) + R_2(t) \\ &\quad +D(t)] + (\mu - \delta)D(t) \\ \frac{dN(t)}{dt} &= \Pi - \mu N(t) + (\mu - \delta)D(t), \qquad \text{since} \qquad \mu < \delta. \end{aligned} \quad (2.3)$$

Note that the natural death rate is lower than EVD induced death rate since EVD case fatality rates are known to varied from 25% to 90% in all EVD outbreaks [44]. These numbers are higher than the natural death rates, hence $\mu < \delta$.

Thus,

$$\Pi - (\mu+\delta)N(t) \leq \frac{dN(t)}{dt} \leq \Pi - \mu N(t),$$

Hence,

$$\frac{\Pi}{(\mu+\delta)} \leq \liminf_{t\to\infty} N(t) \leq \limsup_{t\to\infty} N(t) \leq \frac{\Pi}{\mu},$$

as required. □

2.1.1. Invariant regions

The Ebola model (2.1) will be analyzed in a biologically-feasible region as follows. Consider the feasible region

$$\Gamma \subset \mathbb{R}^7_+$$

with,

$$\Gamma = \left\{ S(t), E(t), I_E(t), I_L(t), R_1(t), R_2(t), D(t) \quad : N_H(t) \leq \frac{\Pi}{\mu} \right\}.$$

The following steps are followed to establish the positive invariance of Γ (i.e., solutions in Γ remain in Γ for all $t > 0$). The rate of change of the total population is obtained by adding the components of the model (2.1) and using (2.3) gives

$$\frac{dN}{dt} = \Pi - \mu N(t) + (\mu - \delta)D(t).$$

Thus,

$$\frac{dN(t)}{dt} \leq \Pi - \mu N(t).$$

A standard comparison theorem [27] can then be used to show that $N(t) \leq N(0)e^{-\mu t} + \frac{\Pi}{\mu}(1 - e^{-\mu t})$, in particular, $N(t) \leq \frac{\Pi}{\mu}$, if $N(0) \leq \frac{\Pi}{\mu}$. Thus, the region Γ is positively-invariant. Hence, it is sufficient to consider the dynamics of the flow generated by (2.1) in Γ. In this region, the model is epidemiologically and mathematically well-posed [24]. Thus, every solution of the model (2.1) with initial conditions in Γ remains in Γ for all $t > 0$. Therefore, the Γ-limit sets of the system (2.1) are contained in Γ. This result is summarized below.

Lemma 2. *The region $\Gamma \subset \mathbb{R}^7_+$ is positively-invariant for the basic model (2.1) with non-negative initial conditions in $\mathbb{R}^7_+$*

In the next section the conditions for the stability of the disease-free equilibrium of the Ebola model (2.1) are explored.

3. Analysis of the model

The Ebola model (2.1) with relapse and reinfection is now analyzed to gain insight into its dynamical features.

3.1. Stability of the disease-free equilibrium (DFE)

The disease free equilibrium (DFE) of model (2.1) is obtained by setting the right hand sides of the model equations to zero and it is given by:

$$\mathcal{E}_0 = (S^*, E^*, I_E^*, I_L^*, R_1^*, R_2^*, D^*) = \left(\frac{\Pi}{\mu}, 0, 0, 0, 0, 0, 0\right).$$

The local asymptotic stability of $\mathcal{E}_0$ can be established using the next generation operator method on system (2.1). Taking the infected compartments $(E^*, I_E^*, I_L^*, R_1^*, R_2^*, D^*)$ at the DFE and using the notation in [40], the Jacobian matrices F and V for the new infection terms and the remaining transfer terms are respectively given by,

$$F = \begin{pmatrix} 0 & \beta & \beta & \beta\tau_1 & 0 & \beta\tau_2 \\ 0 & 0 & 0 & 0 & 0 & 0 \\ 0 & 0 & 0 & 0 & 0 & 0 \\ 0 & 0 & 0 & 0 & 0 & 0 \\ 0 & 0 & 0 & 0 & 0 & 0 \\ 0 & 0 & 0 & 0 & 0 & 0 \end{pmatrix} \text{ and}$$

$$V = \begin{pmatrix} k_1 & 0 & 0 & 0 & 0 & 0 \\ -\sigma & k_2 & 0 & -\rho & 0 & 0 \\ 0 & -\alpha & k_3 & 0 & 0 & 0 \\ 0 & 0 & -h\gamma & k_4 & 0 & 0 \\ 0 & 0 & 0 & -\xi & \mu & 0, \\ 0 & 0 & -(1-h)\gamma & 0 & 0 & \delta \end{pmatrix},$$

where $k_1 = \sigma + \mu,\ k_2 = \alpha + \mu,\ k_3 = \gamma + \mu,\ k_4 = \xi + \rho + \mu$.

It follows that the *basic reproduction number* of the model (2.1), denoted by $\mathcal{R}_0$, is given by;

$$\mathcal{R}_0 = \rho(FV^{-1}) = \frac{\beta\sigma[k_4\delta(k_3+\alpha) + \alpha\gamma[\delta h\tau_1 + (1-h)k_4\tau_2]]}{k_1\delta(k_2k_3k_4 - h\alpha\gamma\rho)} \tag{3.1}$$

The epidemiological quantity, $\mathcal{R}_0$ measures the average number of Ebola cases by a typical Ebola-infected individual (living or dead) introduced into a completely-susceptible human population [5,18,24,40]. Thus, EBOV can be effectively-controlled in the community if the threshold quantity ($\mathcal{R}_0$) can be reduced to (and maintained at) a value less than unity (i.e. $\mathcal{R}_0 < 1$).

3.1.1. The impact of relapse on the reproduction number

Differentiating the *basic reproduction number*, $\mathcal{R}_0$, given in (3.1), partially with respect to the relapse parameter ρ gives

$$\frac{\partial\mathcal{R}_0}{\partial\rho} = \frac{h\beta\sigma\alpha\gamma[k_3\delta(\xi+\mu-\tau_1k_2) + \delta\alpha(\xi+\mu+h\gamma\tau_1) + (1-h)\gamma\alpha\tau_2(\xi+\mu)]}{k_1\delta(k_2k_3k_4 - h\alpha\gamma\rho)^2} > 0.$$

Hence, the *basic reproduction number*, $\mathcal{R}_0$, is an increasing function of the relapse parameter ρ. This implies that the *basic reproduction number* increases with increasing value of the relapse parameter ρ.

Furthermore, taking the limit of the *basic reproduction number*, $\mathcal{R}_0$, as $\rho \to \infty$, gives

$$\lim_{\rho\to\infty} \mathcal{R}_0 = \frac{\beta\sigma[\alpha(1-h)\gamma\tau_2 + \delta(\alpha+k_3)]}{k_1\delta(k_2k_3 - \alpha\gamma h)},$$

this indicates that as more and more individuals experience relapse (i.e. ρ gets large), the value of the *basic reproduction number*, $\mathcal{R}_0$, gets bigger making control efforts to curtail the disease more challenging.

3.2. Existence of endemic equilibrium point (EEP)

Let $\mathcal{E}_1 = (S^{**}, E^{**}, I_E^{**}, I_L^{**}, R_1^{**}, R_2^{**}, D^{**})$ be any arbitrary equilibrium of the Ebola model (2.1). Conditions for the existence of equilibria for which Ebola is endemic in the community (where at least one of the infected variables is non-zero) can be obtained as follows. Let

$$\lambda^{**} = \frac{\beta(I_E^{**} + I_L^{**} + \tau_1R_1^{**} + \tau_2D^{**})}{S^{**} + E^{**} + I_E^{**} + I_L^{**} + R_1^{**} + R_2^{**} + D^{**}} \tag{3.2}$$

be the associated force of infection for Ebola at endemic steady-state. Setting the right-hand sides of the model to zero gives the

Table 2
Number of possible positive real roots of $f(x)$ when $\mathcal{R}_0 < 1$ and $\mathcal{R}_0 > 1$.

Cases	c_2	c_1	c_0	$\mathcal{R}_0$	Number of sign changes	No of possible positive real roots (endemic equilibrium)
1	+	+	+	$\mathcal{R}_0 < 1$	0	0
	+	+	–	$\mathcal{R}_0 > 1$	1	1
2	+	–	+	$\mathcal{R}_0 < 1$	2	0,2
	+	–	–	$\mathcal{R}_0 > 1$	1	1

following expressions (in terms of λ^{**}):

$$
\begin{aligned}
S^{**} &= \frac{\Pi}{\lambda^{**}+\mu}, \quad E^{**} = \frac{\lambda^{**}\Pi}{k_1(\lambda^{**}+\mu)}\\
I_E^{**} &= \frac{\sigma\lambda^{**}\Pi k_3k_4}{k_1(k_2k_3k_4\lambda^{**}+k_2k_3k_4\mu-h\rho\gamma\alpha\lambda^{**}-h\rho\gamma\alpha\mu)}\\
I_L^{**} &= \frac{\alpha\sigma\lambda^{**}\Pi k_4}{k1(k_2k_3k_4\lambda^{**}+k_2k_3k_4\mu-h\rho\gamma\alpha\lambda^{**}-h\rho\gamma\alpha\mu)}\\
R_1^{**} &= \frac{h\gamma\alpha\sigma\lambda^{**}\Pi}{k1(k_2k_3k_4\lambda^{**}+k_2k_3k_4\mu-h\rho\gamma\alpha\lambda^{**}-h\rho\gamma\alpha\mu)}\\
R_2^{**} &= \frac{h\varepsilon\gamma\alpha\sigma\lambda^{**}\Pi}{k_1\mu(k_2k_3k_4\lambda^{**}+k_2k_3k_4\mu-h\rho\gamma\alpha\lambda^{**}-h\rho\gamma\alpha\mu)}\\
D^{**} &= \frac{(1-h)\gamma\alpha\sigma\lambda^{**}\Pi k_4}{k_1\delta(k_2k_3k_4\lambda^{**}+k_2k_3k_4\mu-h\rho\gamma\alpha\lambda^{**}-h\rho\gamma\alpha\mu)}.
\end{aligned}
\tag{3.3}
$$

Substituting the expressions in (3.3) into the equations in (3.2), and simplifying, leads to the following quadratic equation

$$a_2(\lambda^{**})^2 + a_1\lambda^{**} + a_0(1-\mathcal{R}_0) = 0, \tag{3.4}$$

where

$$
\begin{aligned}
a_2 &= \mu k_3\sigma\delta\varepsilon + \mu\alpha\gamma(1-h)\sigma\epsilon + \mu\delta k_2k_3\varepsilon + \mu\alpha\sigma\delta\varepsilon,\\
a_1 &= \mu\delta k_3k_4(k_2+\sigma) + \mu\alpha\sigma k_4[\gamma(1-h)+\delta] + h\alpha\gamma\delta(\sigma\xi-\mu\rho)\\
&\quad +\mu\delta(h\alpha\gamma\sigma - h\alpha\gamma\sigma\varepsilon + k_1k_2k_3\varepsilon)\\
&\quad -\sigma\beta\mu[\alpha\delta\varepsilon + k_3\delta\varepsilon + (1-h)\tau_2\gamma\alpha\varepsilon],\\
a_0 &= k_1\mu\delta(k_2k_3k_4 - h\gamma\alpha\rho).
\end{aligned}
$$

From (3.4), it can easily be seen that $a_2 > 0$. Further, $a_0(1-\mathcal{R}_0) < 0$ whenever $\mathcal{R}_0 > 1$. Thus, the number of possible positive real roots the polynomial (3.4) can have depends on the signs of a_1. This can be analyzed using the Descartes Rule of Signs on the quadratic polynomial $g(x) = c_2x^2 + c_1x + c_0$, given in (3.4) (with $x = \lambda^{**}, c_2 = a_2, \ c_1 = a_1, \ c_0 = a_0(1-\mathcal{R}_0)$). The various possibilities for the roots of $g(x)$ are tabulated in Table 2.

The following results (Theorem 1 and Lemma 3) follow from the various possible combinations for the roots of $f(x)$, in Table 2.

Theorem 1. *The Ebola model (2.1) has a unique endemic equilibrium if $\mathcal{R}_0 > 1$ and whenever Cases 1and 2 are satisfied.*

The existence of multiple endemic equilibria when $\mathcal{R}_0 < 1$ (shown in Table 2) indicates the possibility of backward bifurcation [1,2,7,8,19,47], a phenomenon where the disease-free equilibrium co-exist with a stable endemic equilibrium when the associated reproduction number ($\mathcal{R}_0$) is less than one. This is further explored in Section 3.3 below. To the author's knowledge, this is, the first time backward bifurcation phenomenon has been established in Ebola transmission dynamics.

Table 3
Values of parameters of the model (2.1).

Parameter	Values	References
β	0.3045/day	[3]
Π	400/day	[3]
μ	0.00004/day	[3,15,31]
τ	0.21/day	[3,33]
ρ	Variable	
σ	0.5239/day	[3]
α	0.5472/day	[3]
h	0.48/day	[3,4,26]
ε	Variable	
γ	0.5366/day	[3]
δ	0.5/day	[3,26]

Lemma 3. *The Ebola model (2.1) has at least one positive endemic equilibrium whenever $\mathcal{R}_0 > 1$, and could have zero or two positive endemic equilibria whenever $\mathcal{R}_0 < 1$.*

3.3. Bifurcation analysis

Most mathematical disease transmission models typically undergo at $\mathcal{R}_0 = 1$, a simple transcritical bifurcation (that is, an exchange of stability from the DFE to an endemic equilibrium). The Ebola model (2.1) with relapse and reinfection is investigated for the possibility of backward bifurcation [1,2,7,8,19,47]. The epidemiological implication of this phenomenon is that it is no longer sufficient for the reproduction number to be less than one to guarantee disease elimination since the effective control (or elimination) is now dependent on the initial size of the sub-populations. Thus, it is imperative to understand the consequence of relapse and reinfection on Ebola transmission. Hence, the possibility of the backward bifurcation phenomenon of Ebola model (2.1) with relapse and reinfection is explored using the center manifold theory [8], as described in [9] (Theorem 4.1).

Theorem 2. *The Ebola model (2.1) undergoes backward bifurcation at $\mathcal{R}_0 = 1$ whenever the inequality;*

$$a > 0,$$

holds; where,

$$
\begin{aligned}
a &= v_2\sum_{i,j=1}^{6} w_iw_j\frac{\partial^2 f_2}{\partial x_i\partial x_j} + v_5\sum_{i,j=1}^{6} w_iw_j\frac{\partial^2 f_5}{\partial x_i\partial x_j},\\
&= \frac{\beta(w_3+w_4+w_5\tau_1+w_7\tau_2)[\varepsilon w_5(v_2-v_5) - v_2(w_2+w_3+w_4+w_5+w_6)]}{x_1^*}.
\end{aligned}
$$

The proof of Theorem 2 is given in Appendix A. The backward bifurcation property of the model (2.1) is illustrated by simulating the model using a set of parameter values given in Table 3 (such that the bifurcation parameters take the values $a = 0.8377 \times 10^{-3} > 0$ and $b = 2.3025 > 0$, respectively). The backward bifurcation phenomenon of the model (2.1) makes the effective control of the Ebola virus disease in the population difficult; since, in this

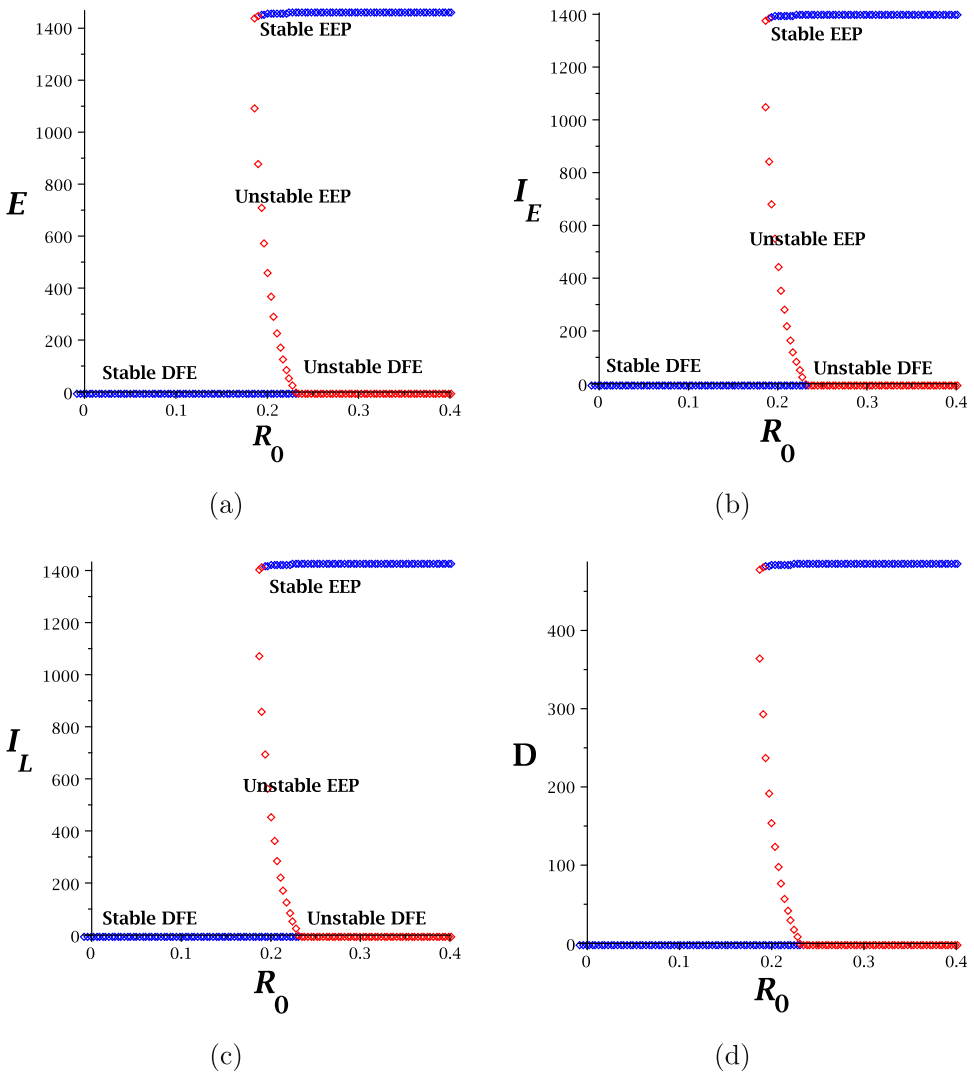

Fig. 2. Backward bifurcation plot of the Ebola model (2.1) as a function of time. (a) The exposed Ebola-infected individuals. (b) The symptomatic living Ebola-infected individuals in the early infection stage. (c) The symptomatic living Ebola-infected individuals in the late infection stage. (d) The Ebola deceased individuals. Parameter values used are as given in Table 3.

case, disease control when $\mathcal{R}_0 < 1$ is dependent on the initial sizes of the sub-populations of the model (2.1). This phenomenon is illustrated numerically in Fig. 2(a)–(d) for the exposed individuals, symptomatic living Ebola-infected individuals in the early and late infection stages and Ebola deceased individuals respectively.

Remark 1. The values of the parameters given in Table 3 were estimated using the 2014 Ebola outbreak data for Guinea [3]. The data was from March 22, to August 29, 2014 [3].

3.3.1. The impact of relapse and reinfection on backward bifurcation.
It should first be noted that if $\varepsilon = 0$, then, the expression for the bifurcation coefficient, a, given in (A-3), reduces to

$$a = \frac{-2\beta v_2(w_2 + w_3 + w_4 + w_5 + w_6)(w_3 + w_4 + w_5\tau_1 + w_7\tau_2)}{x_1} < 0, \tag{3.5}$$

since v_2, w_2, w_3, w_4, w_5, w_6, $w_7 > 0$. Thus, the backward bifurcation phenomenon of the Ebola model (2.1) with relapse and reinfection will not occur if $\varepsilon = 0$ (i.e., the Ebola model will not undergo backward bifurcation in the absence of reinfection).

Furthermore, the impact of the reinfection parameter (ε) on the backward bifurcation is assessed by carrying out an analysis on the bifurcation coefficient, a, as follows. Differentiating a, given in (A-3), partially with respect to reinfection parameter ε gives

$$\frac{\partial a}{\partial \varepsilon} = \frac{2\beta\alpha h\gamma[\gamma\alpha[h\tau_1\delta + (1-h)\tau_2 k_4] + \delta k_4(\alpha + k_3)](\sigma k_4 - \beta\tau_1\sigma - \rho k_1)}{k_1 k_3^2 k_4^3 \delta x_1^*}.$$

Hence, the bifurcation coefficient, a, is an increasing function of reinfection parameter ε provided $\sigma k_4 - \beta\tau_1\sigma - \rho k_1 > 0$. Thus, the feasibility of backward bifurcation occurring increases with increasing values of reinfection parameter ε (because increasing the value of the bifurcation coefficient, a, particularly from negative to positive values, increases the likelihood of the occurrence of backward bifurcation).

Differentiating the bifurcation coefficient, a, given in (A-3), partially with respect to the relapse parameter ρ gives

$$\frac{\partial a}{\partial \rho} = \frac{2h\beta\gamma\alpha}{k_1^2 k_3^2 k_4^4 \mu\delta x_1^*}\Big\{[k_4[(1-h)\tau_2\gamma\alpha + (k_3\delta + \delta\alpha)] + h\delta\tau_1\gamma\alpha]$$
$$[2\mu\sigma\beta\tau_1(\varepsilon k_1 + k_4) + \mu\varepsilon(\rho - \mu - \xi)k_1^2$$

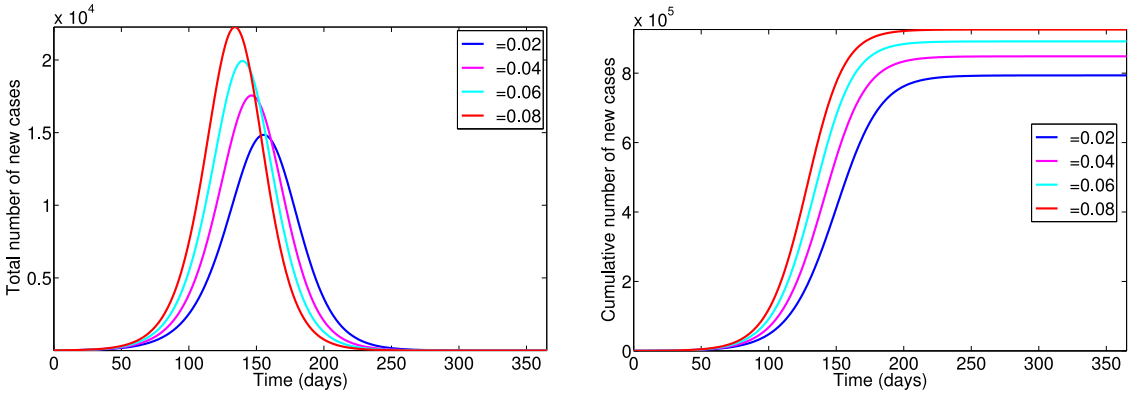

Fig. 3. Simulation of the Ebola model (2.1) as a function of time with different values of $\rho = 0.02,\ 0.04,\ 0.06,\ 0.08$. (a) Total number of Ebola new cases. (b) Cumulative number of Ebola new cases. Parameter values used are as given in Table 3.

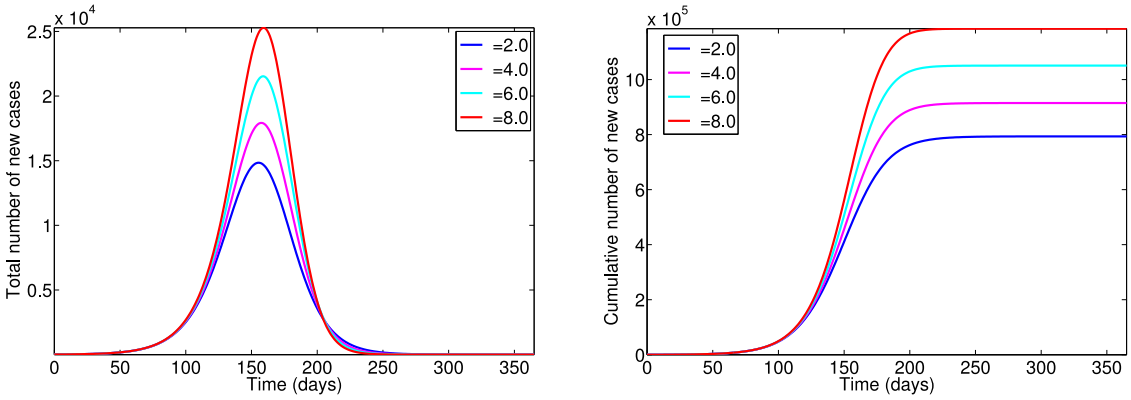

Fig. 4. Simulation of the Ebola model (2.1) as a function of time with different values of $\varepsilon = 1.0,\ 2.0,\ 4.0,\ 8.0$. (a) Total number of Ebola new cases. (b) Cumulative number of Ebola new cases. Parameter values used are as given in Table 3.

$$
\begin{aligned}
&+\sigma(\mu+\xi-\mu\varepsilon)k_1k_4]\\
&+h\delta\tau_1\gamma\alpha[\sigma(\mu+\xi-\mu\varepsilon)k_1k_4+\mu\varepsilon\rho k_1^2+\mu\sigma\varepsilon\beta\tau_1k_1]\\
&+\delta(k_3+\alpha)k_1k_4^2\mu\tau_1\sigma\Big\} > 0.
\end{aligned}
$$

Thus, the backward bifurcation coefficient, a, is an increasing function of the relapse parameter ρ. Hence, the possibility of backward bifurcation occurring increases with increasing relapse parameter ρ rate (i.e., as more individuals experience relapse of the disease, this increases the likelihood of the occurrence of backward bifurcation).

4. Numerical simulations

In this section, the Ebola model (2.1) is simulated as a function of time by varying the relapse parameter (ρ) for, say, $\rho = 0.2, 0.4, 0.6, 0.8$, with the other parameters given in Table 3 kept constant. We observed from Fig. 3(a) that as ρ increases, the total number of new cases of Ebola-infected individuals increases; however, the infection peak time decreases with increasing values of ρ. A similar observation is made for the cumulative number of new cases in Fig. 3(b). It should be noted that model (2.1) is without any interventions (pharmaceutical or otherwise), hence the high number of cases.

The Ebola model (2.1) is also simulated as a function of time by varying the reinfection parameter (ε) in Fig. 4. We observed that both total and cumulative numbers of new cases of Ebola-infected individuals increase as ε increases.

Table 4
Simulation results of the total number of new cases of the Ebola model (2.1) at peak time for different values of ρ and ε.

ρ	Total number of new cases	ε	Total number of new cases
0.02	1.480411×10^4	2.0	1.480411×10^4
0.04	1.751013×10^4	4.0	1.782941×10^4
0.06	1.989794×10^4	6.0	2.136298×10^4
0.08	2.222001×10^4	8.0	2.503305×10^4

In Table 4 (see also Figs. 3(a) and 4(a)) we compare the total number of infected new cases at the peak time for various values of ρ and ε, we observed that higher number of reinfection cases (i.e., increasing ε) lead to more number of new cases in comparison to the total number of new cases due to relapse (i.e., increasing ρ). However, when the reinfection parameter is reduced by 100% and relapse parameter increased by 100%, we observed a reversed trend, where more new cases are generated with increasing relapse and fewer cases with reducing reinfection, see Table 5.

4.1. Model comparisons

As stated in Section 2 above, the Ebola transmission model (2.1) is an extension of numerous published models (e.g., those in [4,16] and the pre-intervention model in [3]) by (*inter alia*):

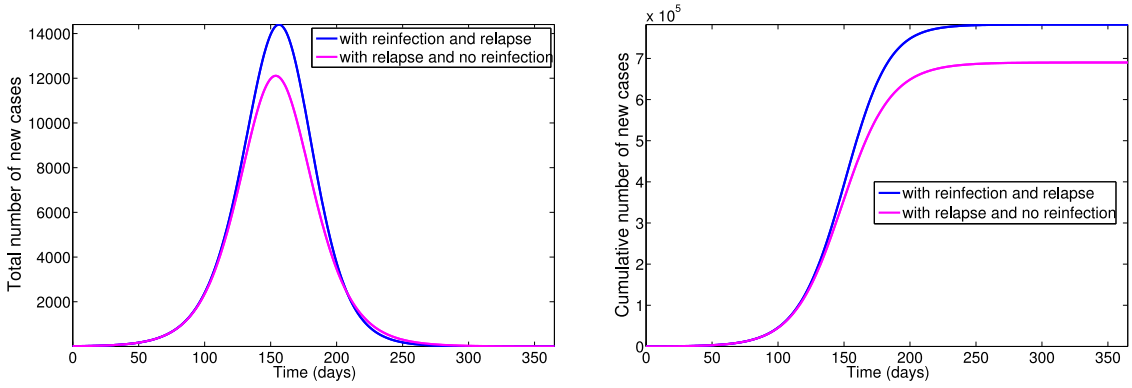

Fig. 5. Simulation of the Ebola model (2.1) with and without disease relapse using parameter values in Table 3. (a) Total number of Ebola new cases. (b) Cumulative number of Ebola new cases.

Table 5
Simulation results of the total number of new cases of the Ebola model (2.1) at peak time for different values of ρ and ε.

ρ	Total number of new cases	ε	Total number of new cases
0.2	3.234656×10^4	0.02	1.239408×10^4
0.4	4.228694×10^4	0.04	1.241560×10^4
0.6	4.831354×10^4	0.06	1.243690×10^4
0.8	5.236526×10^4	0.08	1.245891×10^4

Table 6
Simulation results of the Ebola model (2.1) for the total number of new cases and cumulative numbers of new cases with and without disease relapse and reinfection.

Models	Total number of new cases	Cumulative number of new cases
Reinfection and relapse	1.010184×10^6	1.694367×10^8
Relapse and no reinfection	8.995537×10^5	1.494696×10^8
Reinfection and no relapse	8.900994×10^5	1.459208×10^8
No reinfection and relapse	7.890960×10^5	1.285975×10^8

(i) including relapse of recovered individuals;
(ii) including reinfection of recovered individuals; and
(iii) including two infected and recovered classes.

The impact of the aforementioned extensions on the disease burden is now explored by simulating the model (2.1) in the presence and absence of those extensions using parameter values given in Table 4, these values (except for ρ and ε) were estimated in [3] using Guinea 2014 Ebola Outbreak data.

4.1.1. Effect of incorporating relapse

To assess the impact of incorporating disease relapse on Ebola transmission dynamics, we compare the model (2.1) with a version that does not include disease relapse (that is, we consider the model (2.1) with $\rho = 0$). Fig. 5 shows that both the total number and the cumulative number of new cases of infection generated using the model (2.1) exceeds that of the version of the model without disease relapse. This point is further iterated in Table 6 where the version of the model without disease relapse lead to few number of cases. These results indicate that Ebola transmission models that do not incorporate disease relapse in the disease dynamics may under-estimate Ebola disease burden in the community.

4.1.2. Effect of incorporating reinfection

The model (2.1) is simulated with and without reinfection in order to assess the impact of incorporating reinfection of the recovered individuals in the R_1 class. Fig. 6 shows that the version of the model without reinfection of the recovered individuals lead to a fewer number of new cases. This result corroborate with the results shown in Table 6 where both the total number and cumulative number of new cases are less than the numbers obtained for the Ebola model (2.1) with reinfection of the recovered individuals in the R_1 class.

Table 7
Simulation results of the Ebola model (2.1) for the total number of new cases and cumulative numbers of new cases with different infected and recovered classes.

Models	Total number of new cases	Cumulative number of new cases
One recovered class	6.053832×10^5	8.555489×10^7
One infected and recovered classes	9.194400×10	2.992027×10^4

4.1.3. Effect of incorporating different infected and recovered classes

Next, we access the impact of incorporating in the Ebola model only one class of infected and recovered individuals. Comparing the model (2.1) with the version with only one class of recovered individual and with no disease relapse or reinfection. We observe in Fig. 7 that the Ebola model (2.1) lead to more cases of the total number and the cumulative number of new cases (see also Table 7). Thus indicating that the Ebola model with only one recovered class underestimates the number of new cases of infection. Similar behavior is observed for the version of the model with only one infected class of individuals and no disease relapse or reinfection (see Table 7).

5. Assessment of basic control strategies

In order to assess the impact of basic control strategies, results of sensitivity analysis obtained from the pre-intervention model presented in [3], shows that, in the absence of anti-Ebola public health interventions, the parameters that have the most influence on Ebola transmission dynamics are the progression rate of early-symptomatic individuals (α), the effective contact rate (β) and the recovery rate of symptomatic individuals (γ). These results suggest that a strategy that reduces the progression rate of early-symptomatic individuals (decrease α), reduces the risk of acquisition of Ebola infection (reduce β) and increases the recovery rate (increase γ) would be effective in curtailing the spread of the disease. Thus, following the sensitivity analysis results we assess the role of basic (non-pharmaceutical) public health control measures for effective containment of EBOV outbreaks in the presence of disease relapse and reinfection. As in [3], we implement three control

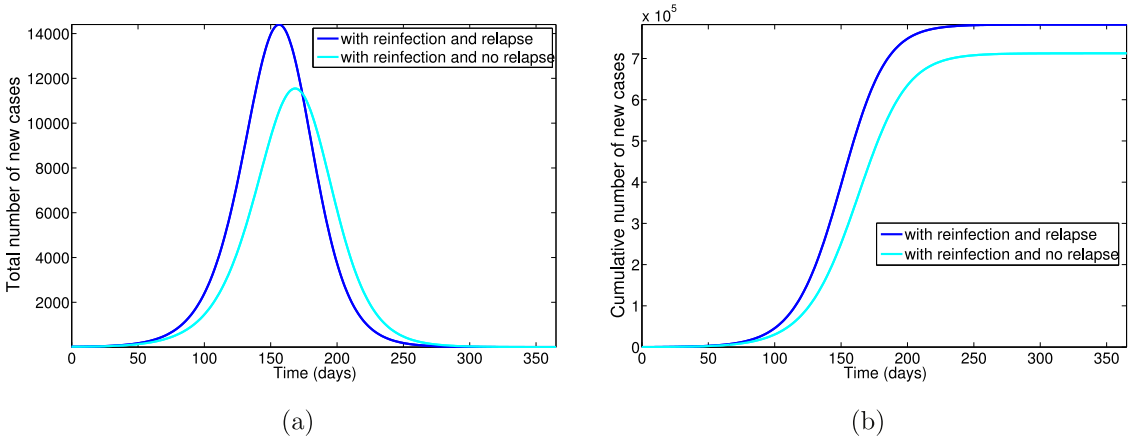

Fig. 6. Simulation of the Ebola model (2.1) with and without disease reinfection using parameter values in Table 3. (a) Total number of Ebola new cases. (b) Cumulative number of Ebola new cases.

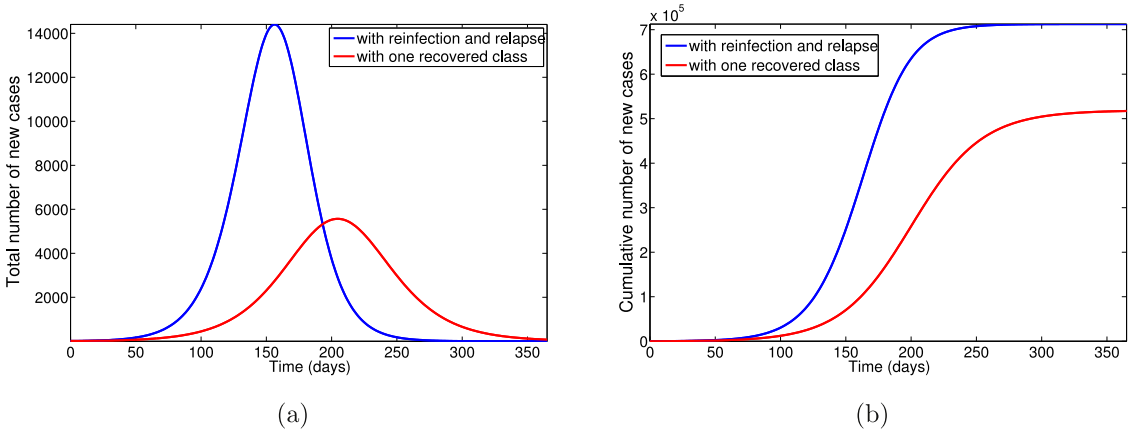

Fig. 7. Simulation of the Ebola model (2.1) with one recovered class using parameter values in Table 3. (a) Total number of Ebola new cases. (b) Cumulative number of Ebola new cases.

Table 8
Simulation results of the Ebola model (2.1) at peak time for the total number of new cases and for cumulative numbers of new cases at final time $t = 500$ days using the three control effectiveness levels.

	Low-effectiveness	Moderate-effectiveness	High-effectiveness
Total	31.920489×10^6	8.501749×10^3	1.920612×10^3
Cumulative	8.425225×10^5	6.955933×10^5	3.339088×10^5

effectiveness levels (low, moderate and high) of the basic public health control strategies by adjusting the parameters β (transmission rate) and γ (recovery rate) to reflect these levels. Thus, the following three effectiveness levels are considered:

1. Low-effectiveness strategy: $\beta = 0.3045$/day, $\gamma = 0.5366$/day;
2. Moderate-effectiveness of the personal-protection strategy: $\beta = 0.2436$/day, $\gamma = 0.4293$/day;
3. High-effectiveness of the personal-protection strategy: $\beta = 0.1860$/day, $\gamma = 0.3277$/day.

Fig. 8(a) and (b) depicts the total and cumulative numbers of new cases generated using the three basic public health control effectiveness levels (i.e., low, moderate and high) over a 500-day period (the end of simulation period). A comparison of the three effectiveness levels in Table 8 at the peak time and time $t = 500$ days show that the high-effectiveness levels lead to a dramatic decline in the number of new cases in comparison to the low-effectiveness level. It is worth noting that the moderate-effectiveness level equally leads to a dramatic decline in the number of new cases in comparison to the low-effectiveness level, even though the high-effectiveness level is far more effective in curtailing Ebola burden in the community. Thus, these simulations clearly show that Ebola outbreaks in the presence of disease relapse and reinfections are controllable using basic public health control measures, such as the moderate- and high-effectiveness levels of the control strategy described above.

6. Discussion and conclusions

In this paper, we incorporated disease relapse and reinfection into a deterministic model obtained from [3] for the transmission dynamics of Ebola model in order to study the impact of relapse and reinfection on the virus transmission. The study shows that the disease-free equilibrium of the model is locally-asymptotically stable whenever the associated reproduction number ($\mathcal{R}_0$), is less than unity and unstable otherwise. The *basic reproduction number*, ($\mathcal{R}_0$), is shown to be an increasing function of the relapse parameter ρ. This implies that when a lot of recovered individuals experience relapse, $\mathcal{R}_0$, gets bigger making control efforts to curtail the disease very challenging.

The model is further shown to exhibits in the presence of disease reinfection the phenomenon of backward bifurcation, where the stable disease-free equilibrium co-exists with a stable endemic equilibrium when the associated reproduction number is less than unity. Assessing the impact of reinfection (ε) on the bifurcation coefficient (a) shows that ε is an increasing function of the bifurcation coefficient. This implies that the feasibility of backward bifur-

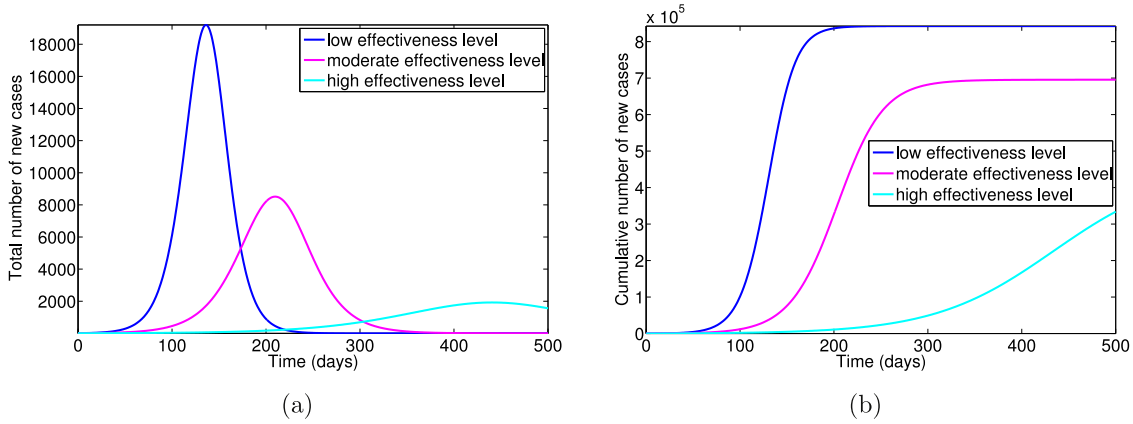

Fig. 8. Simulation of the Ebola model (2.1) as a function of time for various effectiveness levels of the basic public health control strategy. (a) Total number of Ebola new cases. (b) Cumulative number of Ebola new cases. Parameter values used are as given in Table 3.

cation occurring increases with increasing values of the reinfection parameter, ε. Similarly, The possibility of backward bifurcation occurring increases with increasing relapse parameter (ρ), that is, a is an increasing function of ρ. Thus, as more individuals experience disease relapse, the likelihood of the occurrence of backward bifurcation increases. This means that as more individuals in the community experience disease relapse and reinfection, the likelihood of backward bifurcation increases. The implication of this rest in the requirement to eliminate the virus transmission, which now is more than just reducing the reproduction to a value less than unity.

The simulations of the Ebola model (2.1) as a function of time indicate (in the absence of intervention) that both the total and cumulative numbers of new cases of Ebola-infected individuals increases with increasing numbers of relapse and reinfected individuals. The reinfection of the recovered individuals will lead to more cases compare to infection relapse if reinfection rate is greater than relapse rate and *vice versa*. The Ebola model (2.1) extends several existing Ebola transmission models including [3,4,16], by incorporating disease relapse, reinfection of recovered individuals and the inclusion of two infected and recovered classes. We assessed the effect of these extensions using numerical simulations with parameters values estimated using the 2014 Ebola outbreak data from Guinea. We observed that Ebola models which do not incorporate these dynamics may under-estimate Ebola burden in the community. Furthermore, the numerical simulations show the impact of disease relapse which leads to more infected cases compare to the cases with disease reinfection. The simulations further emphasize the impact of the inclusion of both relapse and reinfection in an Ebola transmission model which leads to increase disease burden in the community.

In order to reduce the number of infected cases different parameters values were adjusted using the results obtained from the sensitivity analysis obtained in [3] and three different control effectiveness levels (low, moderate, high) were implemented using both the total and cumulative numbers of new cases of Ebola infections as output measures. The results show that the cumulative number of new cases of infections decreases with increasing effectiveness level, with the high-effectiveness level producing a dramatic reduction in the number of new cases, this is followed by the moderate-effectiveness level. The numerical simulations indicate that the high-effectiveness level is more effective than either the moderate- or low-effectiveness levels; however, it leads to dramatic reduction in the number of new cases. Furthermore, the moderate-effectiveness level is also able to produce a dramatic reduction in disease burden, although not as much as the high-effectiveness level .

Hence, in this paper, we formulated and analyzed a system of ordinary differential equations for transmission dynamics of Ebola virus, incorporated into the model are disease relapse and reinfection. Some of theoretical, epidemiological and numerical findings of this study are summarized below:

(i) The Ebola model (2.1) is locally-asymptotically stable (LAS) when $\mathcal{R}_0 < 1$ and unstable when $\mathcal{R}_0 > 1$.
(ii) The *basic reproduction number*, ($\mathcal{R}_0$), is an increasing function of the relapse parameter ρ. When more recovered individuals experience relapse, $\mathcal{R}_0$, gets bigger. Thus, making control efforts to curtail the disease very challenging.
(iii) The model exhibits in the presence of disease reinfection the phenomenon of backward bifurcation, where the stable disease-free equilibrium co-exists with a stable endemic equilibrium when the associated reproduction number is less than unity.
(iv) The feasibility of backward bifurcation occurring increases with increasing values of reinfection parameter ε and the possibility of backward bifurcation occurring increases with increasing relapse parameter ρ rate.
(v) The total number of new cases of Ebola-infected individuals increases with increasing values of the relapse and reinfection parameters (i.e., ρ and ε). And reinfection will lead to more cases compare to infection relapse if reinfection rate is greater than relapse rate and *vice versa*.
(vi) The Ebola model (2.1) extends several existing Ebola transmission models, notably by incorporating disease relapse, reinfection of recovered individuals in the R_1 class and the inclusion of only one infected and recovered classes without disease relapse and reinfection. The effect of these extensions was assessed using numerical simulations, from which we observed (based on the parameter values and ranges used in the simulations) that Ebola models which does not incorporate these dynamics may under-estimate Ebola burden in the community.
(vii) Numerical simulations indicate that the high-effectiveness level is more effective than either the moderate- or low-effectiveness levels; this is followed by the moderate-effectiveness level.

Acknowledgment

The author acknowledges the anonymous referees for their constructive comments and suggestions that have greatly improved the results of this work.

Appendix A. Proof of Theorem 2

Proof. The prove of Theorem 2 uses of Center Manifold theory [8,9]. For convenience, we makes the following transformations and change of variables. Let, $S(t) = x_1$, $E(t) = x_2$, $I_E(t) = x_3$, $I_L(t) = x_4$, $R_1(t) = x_5$, $R_2(t) = x_6$ $D(t) = x_7$. Using the vector notation $\mathbf{x} = (x_1, x_2, x_3, x_4, x_5, x_6, x_7)^T$, the malaria vaccination model (2.1) can be written in the form $\frac{d\mathbf{x}}{dt} = \mathbf{m}(\mathbf{x})$, where $\mathbf{f} = (f_1, f_2, f_3, f_4, f_5, f_6, f_7)^T$, as follows:

$$\begin{aligned}
\frac{dx_1}{dt} &= f_1 = \Pi - \frac{\beta(x_3 + x_4 + +\tau_1 x_5 + \tau_2 x_7)x_1}{x_1 + x_2 + x_3 + x_4 + x_5 + x_6 + x_7} - \mu x_1,\\
\frac{dx_2}{dt} &= f_2 = \frac{\beta(x_3 + x_4 + \tau_1 x_5 + \tau_2 x_7)x_1}{x_1 + x_2 + x_3 + x_4 + x_5 + x_6 + x_7}\\
&\quad + \frac{\varepsilon\beta(x_3 + x_4 + \tau_1 x_5 + \tau_2 x_7)x_5}{x_1 + x_2 + x_3 + x_4 + x_5 + x_6 + x_7} - k_1 x_2,\\
\frac{dx_3}{dt} &= f_3 = \sigma x_2 - k_2 x_3 + \rho x_5,\\
\frac{dx_4}{dt} &= f_4 = \alpha x_3 - k_3 x_4,\\
\frac{dx_5}{dt} &= f_5 = h\gamma x_4 - k_4 x_5 - \frac{\varepsilon\beta(x_3 + x_4 + \tau_1 x_5 + \tau_2 x_7)x_5}{x_1 + x_2 + x_3 + x_4 + x_5 + x_6 + x_7},\\
\frac{dx_6}{dt} &= f_6 = \xi x_5 - \mu x_6,\\
\frac{dx_7}{dt} &= f_7 = H\gamma x_4 - \delta x_7.
\end{aligned} \tag{A-1}$$

The Jacobian of the transformed Ebola model (A-1) at the DFE $\mathcal{E}_0$ is given as

$$\mathcal{J}(\mathcal{E}_0) = \begin{pmatrix}
-\mu & 0 & -\beta & -\beta & -\beta\tau_1 & 0 & -\beta\tau_2\\
0 & -k_1 & \beta & \beta & \beta\tau_1 & 0 & \beta\tau_2\\
0 & \sigma & -k_2 & 0 & \rho & 0 & 0\\
0 & 0 & \alpha & -k_3 & 0 & 0 & 0\\
0 & 0 & 0 & h\gamma & -k_4 & 0 & 0\\
0 & 0 & 0 & 0 & \xi & -\mu & 0\\
0 & 0 & 0 & (1-h)\gamma & 0 & 0 & -\delta
\end{pmatrix},$$

Consider the case when $\mathcal{R}_0 = 1$. Suppose, further, that β is chosen as a bifurcation parameter. Solving (3.1) for β from $\mathcal{R}_0 = 1$ gives $\beta = \beta^*$.

$$\beta^* = \frac{k_1\delta(k_2k_3k_4 - \alpha h\gamma\rho)}{\sigma[\delta k_4(k_3 + \alpha) + \gamma\alpha[\tau_1 h\delta + \tau_2(1-h)k_4]]} \tag{A-2}$$

The transformed system (A-1) at the DFE evaluated at $\beta = \beta^*$ has a simple zero eigenvalue (and all other eigenvalues have negative real parts). Hence, the Center Manifold theory [8] can be used to analyze the dynamics of (A-1) near $\beta = \beta^*$. In particular, the theorem in [9] (see also [8,19,40]) is used. To apply the theorem, the following computations are necessary.

Eigenvectors of $J(\mathcal{E}_0)|_{\beta=\beta^*}$:

The Jacobian of the transform malaria vaccination model (A-1) at $\beta = \beta^*$, denoted by $J(\mathcal{E}_0)|_{\beta=\beta^*}$, has a left and right eigenvectors (associated with the zero eigenvalue) given by

$$\mathbf{w} = (w_1, w_2, w_3, w_4, w_5, w_6)^T, \quad \text{and} \quad \mathbf{v} = (v_1, v_2, v_3, v_4, v_5, v_6)^T,$$

where,

$$\begin{aligned}
w_1 &= -\frac{(\beta w_3 + \beta w_4 + \beta\tau_1 w_5 + \beta\tau_2 w_7)}{\mu},\\
w_2 &= \frac{(\beta w_3 + \beta w_4 + \beta\tau_1 w_5 + \beta\tau_2 w_7)}{k_1},\\
w_3 &= w_3 > 0, \quad w_4 = \frac{\alpha w_3}{k_3}, \quad w_5 = \frac{h\gamma w_4}{k_4},\\
w_6 &= \frac{\xi w_5}{\mu}, \quad w_7 = \frac{(1-h)\gamma w_4}{\delta}.
\end{aligned}$$

and

$$\begin{aligned}
v_1 &= 0, \quad v_6 = 0, \quad v_2 = \frac{v_3\sigma}{k_1}, \quad v_3 = v_3 > 0,\\
v_4 &= \frac{[-\beta v_1 + \beta v_2 + h\gamma v_5 + (1-h)\gamma v_7]}{k_3},\\
v_5 &= \frac{-\beta\tau_1 v_1 + \beta\tau_1 v_2 + \rho v_3 + \xi v_6}{k_4},\\
v_7 &= \frac{-\beta\tau_2 v_1 + \beta\tau_2 v_2}{\delta}.
\end{aligned}$$

Computations of bifurcation coefficients a and b:

The application of the theorem involves the computation of two bifurcation coefficients a and b, which are obtained after some algebraic manipulations as follow:

$$\begin{aligned}
a &= v_2 \sum_{i,j=1}^{6} w_i w_j \frac{\partial^2 f_2}{\partial x_i \partial x_j} + v_5 \sum_{i,j=1}^{6} w_i w_j \frac{\partial^2 f_5}{\partial x_i \partial x_j},\\
&= \frac{\beta(w_3 + w_4 + w_5\tau_1 + w_7\tau_2)[\varepsilon w_5(v_2 - v_5) - v_2(w_2 + w_3 + w_4 + w_5 + w_6)]}{x_1^*}.
\end{aligned} \tag{A-3}$$

Furthermore,

$$b = v_2 \sum_{i=1}^{6} w_i \frac{\partial^2 f_2}{\partial x_i \partial \beta^*} = v_2(w_3 + w_4 + w_5\tau_1 + w_7\tau_2) > 0.$$

Thus, the transformed model (A-1) using Theorem 4.1 of [9] undergoes backward bifurcation at $\mathcal{R}_0 = 1$ whenever the following inequality holds:

$$a > 0. \tag{A-4}$$

□

References

[1] F.B. Agusto, A.B. Gumel, S. Lenhart, A. Odoi, Mathematical analysis of the transmission dynamics of bovine tuberculosis model, J. Math. Methods Appl. Sci. 34 (2011) 1873–1887.
[2] F.B. Agusto, A.B. Gumel, Qualitative dynamics of lowly- and highly-pathogenic avian influenza strains, Math. Biosci. 243 (2) (2013) 147–162.
[3] F.B. Agusto, M.I. Teboh-Ewungkem, A.B. Gumel, Mathematical assessment of the role of traditional belief systems and customs and health-care settings in the transmission dynamics of the 2014 ebola outbreaks, BMC Med. 13 (2015) 96.
[4] C.L. Althaus, Estimating the Reproduction Number of Ebola Virus (EVOB) During the 2014 Outbreak in West Africa, 1st ed., PLOS Currents Outbreaks, 2014.
[5] R.M. Anderson, R. May, Infectious Diseases of Humans, Oxford University Press, New York, 1991.
[6] D.G. Bausch, J.S. Towner, S.F. Dowell, F. Kaducu, M. Lukwiya, A. Sanchez, et al., Assessment of the risk of ebola virus transmission from bodily fluids and fomites, J. Infect. Dis. 196 (Suppl. 2) (2007) S142–147.
[7] F. Brauer, Backward bifurcations in simple vaccination models, J. Math. Anal. Appl. 298 (2) (2004) 418–431.
[8] J. Carr, Applications of Centre Manifold Theory, Springer, 1981.
[9] C. Castillo-Chavez, B. Song, Dynamical models of tuberculosis and their applications, Math. Biosci. Eng. 1 (2) (2004) 361–404.

[10] Centers for Disease Control and Prevention (CDC), Ebola (ebola virus disease): 2014 West Africa outbreak. http://www.cdc.gov/vhf/ebola/outbreaks/2014-west-africa/survivors.html, 2016 (accessed 20.06.16).
[11] Centers for Disease Control and Prevention (CDC), Outbreaks chronology: Ebola hemorrhagic fever. http://www.cdc.gov/vhf/Ebola/resources/outbreak-table.html, 2014 (accessed 25.08.14).
[12] Centers for Disease Control and Prevention (CDC), Ebola hemorrhagic fever. http://www.cdc.gov/vhf/Ebola/, 2014 (accessed 25.08.14).
[13] Centers for Disease Control and Prevention (CDC), Ebola hemorrhagic fever: fact sheet, http://www.cdc.gov/vhf/Ebola/pdf/Ebola-factsheet.pdf, 2015 (accessed 11.09.16).
[14] A.L. Chan, What actually happens when a person is infected with the Ebola virus. http://www.huffingtonpost.com/2014/08/02/Ebola-symptoms-infection-virus_n_5639456.html, 2014.
[15] N. Chitnis, J.M. Cushing, J.M. Hyman, Bifurcation analysis of a mathematical model for malaria transmission, SIAM J. Appl. Math. 67 (2006) 24–45.
[16] G. Chowell, N.W. Hengartner, C. Castillo-Chavez, P.W. Fenimore, J.M. Hyman, The basic reproductive number of Ebola and the effects of public health measures: the cases of Congo and Uganda 28 (2004) 503–522.
[17] G.F. Deen, B. Knust, N. Broutet, F.R. Sesay, P. Formenty, C. Ross, et al., Ebola RNA persistence in semen of ebola virus disease survivors – preliminary report, N. Engl. J. Med. (2015) 1–7.
[18] O. Diekmann, J.A.P. Heesterbeek, J.A.P. Metz, On the definition and computation of the basic reproduction ratio R_0 in models for infectious diseases in heterogeneous populations, J. Math. Biol 28 (1990) 503–522.
[19] J. Dushoff, H. Wenzhang, C. Castillo-Chavez, Backwards bifurcations and catastrophe in simple models of fatal diseases, J. Math. Biol. 36 (1998) 227–248.
[20] F.O. Fasina, A. Shittu, D. Lazarus, O. Tomori, L. Simonsen, C. Viboud, G. Chowell, Transmission dynamics and control of Ebola virus disease outbreak in Nigeria, July to September 2014, Eurosurveillance 19 (40) (2014) 09.
[21] The Guardian, Ebola study finds women in guinea who appear immune to the virus. http://www.theguardian.com/world/2015/oct/15/ebolastudy-finds-women-guinea-appear-immune-virus, 2015.
[22] M. Gupta, S. Mahanty, P. Greer, J.S. Towner, W.J. Shieh, S.R. Zaki, Persistent infection with ebola virus under conditions of partial immunity, J. Virol. 78 (2004) 958–967.
[23] R.T. Heffernan, B. Pambo, R.J. Hatchett, P.A. Leman, R. Swanepoel, R.W. Ryder, Low seroprevalence of IGG antibodies to Ebola virus in an epidemic zone: Ogooue-Ivindo region, Northeastern Gabon, 1997, J. Infect. Dis. 191 (2005) 964–968.
[24] H.W. Hethcote, The mathematics of infectious diseases, SIAM Rev. 42 (4) (2000) 599–653.
[25] B. Kreuels, D. Wichmann, P. Emmerich, J. Schmidt-Chanasit, G. de Heer, S. Kluge, et al., A case of severe Ebola virus infection complicated by gram-negative septicemia, N. Engl. J. Med. 371 (2014) 2394–2401.
[26] J. Legrand, R.F. Grais, P.Y. Boelle, A.J. Valleron, A. Flahaut, Understanding the dynamics of Ebola epidemics, Epidemiol. Infect. 135 (4) (2007) 610–621.
[27] V. Lakshmikantham, S. Leela, A.A. Martynyuk, Stability Analysis of Nonlinear Systems, Marcel Dekker, Inc., New York, Basel, 1989.
[28] E.M. Leroy, S. Baize, V.E. Volchkov, S.P. Fisher-Hoch, M.C. Georges-Courbot, J. Lansoud-Soukate, Human asymptomatic Ebola infection and strong inflammatory response, Lancet 355 (2000) 2210–2215.
[29] C.R. MacIntyre, A.A. Chughtai, Recurrence and reinfection-a new paradigm for the management of ebola virus disease, Int. J. Infect. Dis. 43 (2015) 58–61.
[30] M.I. Meltzer, C.Y. Atkins, S. Santibanez, B. Knust, B.W. Petersen, E.D. Ervin, S.T. Nichol, I.K. Damon, M.L. Washington, Estimating the future number of cases in the ebola epidemic Liberia and Sierra Leone, 2014–2015, Morb. Mortal. Wkly. Rep. 63 (03) (2014) 1–14.
[31] A.M. Niger, A.B. Gumel, Mathematical analysis of the role of repeated exposure on malaria transmission dynamics, Differ. Equ. Dyn. Syst. 16 (2008) 251–287.
[32] H. Nishiura, G. Chowell, Early transmission dynamics of ebola virus disease (EVD), West Africa, Eurosurveillance 19 (36) (2014).
[33] M. Nuño, T.A. Reichert, G. Chowell, A.B. Gumel, Protecting residential care facilities from pandemic influenza, Proc. Natl. Acad. Soc. 105 (30) (2008) 10625–10630.
[34] L.L. Rodriguez, A. De Roo, Y. Guimard, S.G. Trappier, A. Sanchez, D. Bressler, Persistence and genetic stability of ebola virus during the outbreak in kikwit, democratic republic of the congo., J. Infect. Dis. 179 (Suppl. 1) (1995) S170–176.
[35] A.K. Rowe, J. Bertolli, A.S. Khan, R. Mukunu, J.J. Muyembe-Tamfum, D. Bressler, Clinical, virologic, and immunologic follow-up of convalescent ebola hemorrhagic fever patients and their household contacts, kikwit, democratic republic of the congo, J. Infect. Dis. 179 (Suppl. 1) (1999) S28–35.
[36] A. Sobarzo, Y. Eskira, A.S. Herbert, A.I. Kuehne, S.W. Stonier, D.E. Ochayon, et al., Immune memory to sudan virus: comparison between two separate disease outbreaks, Viruses 7 (2015) 37–51.
[37] J.E. Strong, G. Wong, S.E. Jones, A. Grolla, S. Theriault, G.P. Kobinger, et al., Stimulation of ebola virus production from persistent infection through activation of the ras/MAPK pathway, Proc. Natl. Acad. Soc. 105 (2008) 17982–17987.
[38] S. Towers, O. Patterson-Lomba, C. Castillo-Chavez, Temporal Variations in the Effective Reproduction Number of the 2014 West Africa Ebola Outbreak, 1st ed., PLOS Currents Outbreaks, 2014.
[39] X. Qiu, J. Audet, G. Wong, L. Fernando, A. Bello, S. Pillet, et al., Sustained protection against ebola virus infection following treatment of infected nonhuman primates with ZMAb, Sci. Rep. 3 (2013) 3365.
[40] P. van den Driessche, J. Watmough, Reproduction numbers and sub-threshold endemic equilibria for compartmental models of disease transmission, Math. Biosci. 180 (2002) 29–48.
[41] J.B. Varkey, J.G. Shantha, I. Crozier, C.S. Kraft, G.M. Lyon, A.K. Mehta, et al., Persistence of ebola virus in ocular fluid during convalescence, N. Engl. J. Med. 372 (25) (2015) 2423–2427.
[42] World Health Organization (WHO), Ebola virus disease, fact sheet No 103, http://www.who.int/mediacentre/factsheets/fs103/en/, 2015 (assessed 11.09.16).
[43] WHO Ebola Response Team, Ebola virus disease in west Africa the first 9 months of the epidemic and forward projections, N. Engl. J. Med. 371 (2014) 1481–1495, doi:10.1056/NEJMoa1411100.
[44] World Health Organization, Ebola virus disease, fact sheet No 103. http://www.who.int/mediacentre/factsheets/fs103/en/, 2016 (accessed 20.02.16).
[45] World Health Organization, Persistent virus in people recovering from ebola virus disease, http://www.who.int/csr/disease/ebola/virus-persistence/en/, 2016 (accessed 20.02.16).
[46] World Health Organization, Latest ebola outbreak over in liberia; west africa is at zero, but new flare-ups are likely to occur. http://www.who.int/mediacentre/news/releases/2016/ebola-zero-liberia/en/#, 2016 (accessed 20.02.16).
[47] C. Zaleta, J. Velasco-Hernandez, A simple vaccination model with multiple endemic state, Math. Biosci. 164 (2000) 183–201.